Physics Letters B 723 (2013) 54–60

Contents lists available at SciVerse ScienceDirect

Physics Letters B

www.elsevier.com/locate/physletb

A new limit on the CP violating decay $K_S \to 3\pi^0$ with the KLOE experiment

The KLOE-2 Collaboration

D. Babusci [h], D. Badoni [r,s], I. Balwierz-Pytko [g], G. Bencivenni [h], C. Bini [p,q], C. Bloise [h], F. Bossi [h], P. Branchini [u], A. Budano [t,u], L. Caldeira Balkeståhl [w], G. Capon [h], F. Ceradini [t,u], P. Ciambrone [h], F. Curciarello [j,d], E. Czerwiński [g], E. Danè [h], V. De Leo [j,d], E. De Lucia [h], G. De Robertis [b], A. De Santis [p,q], A. Di Domenico [p,q], C. Di Donato [l,m], R. Di Salvo [s], D. Domenici [h], O. Erriquez [a,b], G. Fanizzi [a,b], A. Fantini [r,s], G. Felici [h], S. Fiore [p,q], P. Franzini [p,q], P. Gauzzi [p,q], G. Giardina [j,d], S. Giovannella [h], F. Gonnella [r,s], E. Graziani [u], F. Happacher [h], L. Heijkenskjöld [w], B. Höistad [w], L. Iafolla [h], M. Jacewicz [w], T. Johansson [w], K. Kacprzak [g], A. Kupsc [w], J. Lee-Franzini [h,v], B. Leverington [h], F. Loddo [b], S. Loffredo [t,u], G. Mandaglio [j,d,c], M. Martemianov [k], M. Martini [h,o], M. Mascolo [r,s], R. Messi [r,s], S. Miscetti [h,*], G. Morello [h], D. Moricciani [s], P. Moskal [g], F. Nguyen [u,1], A. Passeri [u], V. Patera [n,h], I. Prado Longhi [t,u], A. Ranieri [b], C.F. Redmer [i], P. Santangelo [h], I. Sarra [h], M. Schioppa [e,f], B. Sciascia [h], M. Silarski [g,*], C. Taccini [t,u], L. Tortora [u], G. Venanzoni [h], W. Wiślicki [x], M. Wolke [w], J. Zdebik [g]

[a] *Dipartimento di Fisica dell'Università di Bari, Bari, Italy*
[b] *INFN Sezione di Bari, Bari, Italy*
[c] *Centro Siciliano di Fisica Nucleare e Struttura della Materia, Catania, Italy*
[d] *INFN Sezione di Catania, Catania, Italy*
[e] *Dipartimento di Fisica dell'Università della Calabria, Cosenza, Italy*
[f] *INFN Gruppo collegato di Cosenza, Cosenza, Italy*
[g] *Institute of Physics, Jagiellonian University, Cracow, Poland*
[h] *Laboratori Nazionali di Frascati dell'INFN, Frascati, Italy*
[i] *Institut für Kernphysik, Johannes Gutenberg Universität Mainz, Germany*
[j] *Dipartimento di Fisica e Scienze della Terra dell'Università di Messina, Messina, Italy*
[k] *Institute for Theoretical and Experimental Physics (ITEP), Moscow, Russia*
[l] *Dipartimento di Fisica dell'Università "Federico II", Napoli, Italy*
[m] *INFN Sezione di Napoli, Napoli, Italy*
[n] *Dipartimento di Scienze di Base ed Applicate per l'Ingegneria dell'Università "Sapienza", Roma, Italy*
[o] *Dipartimento di Scienze e Tecnologie applicate, Università "Guglielmo Marconi", Roma, Italy*
[p] *Dipartimento di Fisica dell'Università "Sapienza", Roma, Italy*
[q] *INFN Sezione di Roma, Roma, Italy*
[r] *Dipartimento di Fisica dell'Università "Tor Vergata", Roma, Italy*
[s] *INFN Sezione di Roma Tor Vergata, Roma, Italy*
[t] *Dipartimento di Matematica e Fisica dell'Università "Roma Tre", Roma, Italy*
[u] *INFN Sezione di Roma Tre, Roma, Italy*
[v] *Physics Department, State University of New York at Stony Brook, USA*
[w] *Department of Physics and Astronomy, Uppsala University, Uppsala, Sweden*
[x] *National Centre for Nuclear Research, Warsaw, Poland*

ARTICLE INFO

Article history:
Received 31 January 2013
Received in revised form 30 April 2013
Accepted 3 May 2013
Available online 9 May 2013
Editor: M. Doser

ABSTRACT

We have carried out a new direct search for the CP violating decay $K_S \to 3\pi^0$ with 1.7 fb^{-1} of e^+e^- collisions collected by the KLOE detector at the Φ-factory DAΦNE. We have searched for this decay in a sample of about 5.9×10^8 $K_S K_L$ events tagging the K_S by means of the K_L interaction in the calorimeter and requiring six prompt photons. With respect to our previous search, the analysis has been improved by increasing of a factor four the tagged sample and by a more effective background rejection of fake K_S tags and spurious clusters. We find no candidates in data and simulated background samples, while we

* Corresponding authors.
E-mail address: michal.silarski@uj.edu.pl (M. Silarski).
[1] Present address: Laboratório de Instrumentação e Física Experimental de Partículas, Lisbon, Portugal.

0370-2693/$ – see front matter
http://dx.doi.org/10.1016/j.physletb.2013.05.008

Keywords:
e^+e^- collisions
DAΦNE
KLOE
Rare K_S decays
CP
CPT

expect 0.12 standard model events. Normalizing to the number of $K_S \to 2\pi^0$ events in the same sample, we set the upper limit on $\mathrm{BR}(K_S \to 3\pi^0) \leqslant 2.6 \times 10^{-8}$ at 90% C.L., five times lower than the previous limit. We also set the upper limit on the η_{000} parameter, $|\eta_{000}| \leqslant 0.0088$ at 90% C.L., improving by a factor two the latest direct measurement.

1. Introduction

The decay $K_S \to 3\pi^0$ violates CP invariance and its observation would be the first example of CP violation in K_S decays. The parameter η_{000}, the ratio of K_S to K_L decay amplitudes, is defined as: $\eta_{000} = A(K_S \to 3\pi^0)/A(K_L \to 3\pi^0) = \epsilon + \epsilon'_{000}$, where ϵ indicates the K_S CP impurity and ϵ'_{000} the contribution of a direct CP-violating term. Since we expect $\epsilon'_{000} \ll \epsilon$ [1], it follows that $\eta_{000} \sim \epsilon$. In the Standard Model, therefore, $\mathrm{BR}(K_S \to 3\pi^0) \sim 1.9 \times 10^{-9}$, to a relative accuracy better than 1%. The observation of such decay remains quite a challenge.

Previous searches follow two alternative methods: via a fit to the interference pattern or via a direct search. The NA48 Collaboration [2] has fit the $K_S/K_L \to 3\pi^0$ interference pattern at small decay times finding $\Re(\eta_{000}) = -0.002 \pm 0.011_{\mathrm{stat}} \pm 0.015_{\mathrm{sys}}$ and $\Im(\eta_{000}) = -0.003 \pm 0.013_{\mathrm{stat}} \pm 0.017_{\mathrm{sys}}$, corresponding to a limit on $\mathrm{BR}(K_S \to 3\pi^0) \leqslant 7.4 \times 10^{-7}$ at 90% C.L. The best upper limit on $\mathrm{BR}(K_S \to 3\pi^0)$ comes from the direct search performed by the KLOE experiment [3] based on 450 pb^{-1} of collision data collected during 2001–2002. KLOE observed 2 candidates, and quoted a limit on $\mathrm{BR}(K_S \to 3\pi^0) \leqslant 1.2 \times 10^{-7}$ at 90% C.L. [4]. In this Letter, we present a twofold improvement of this search based on a four times larger, and independent, data sample collected in 2004–2005 and on improved techniques used for background rejection.

2. The KLOE detector

The KLOE experiment operated from 2000 to 2006 at DAΦNE, the Frascati ϕ-factory. DAΦNE [5] is an e^+e^- collider running at a center-of-mass energy of ~ 1020 MeV, the mass of the ϕ meson. Equal energy positron and electron beams collide at an angle of π-25 mrad, producing ϕ mesons nearly at rest. The detector consists of a large cylindrical Drift Chamber (DC) [6], surrounded by a lead scintillating fiber Electromagnetic Calorimeter (EMC) [7] both immersed in an axial 0.52 T magnetic field produced by a superconducting coil around the EMC. At the beams interaction point, IP, the spherical beam pipe of 10 cm radius is made of a Beryllium–Aluminum alloy of 0.5 mm thickness. Low beta quadrupoles are located inside the detector at a distance of about ± 50 cm from the interaction region. The drift chamber, 4 m in diameter and 3.3 m long, has 12 582 all stereo drift cells with tungsten sense wires and is a really light structure with an average thickness less than 0.1 X_0, having the chamber shell made of carbon fiber-epoxy composite with an internal wall of ~ 1 mm thickness, and filled with a gas mixture of 90% helium, 10% isobutane, to minimize K_S regeneration and photon conversion. The spatial resolutions are $\sigma_{xy} \sim 150$ μm and $\sigma_z \sim 2$ mm. The momentum resolution is $\sigma(p_\perp)/p_\perp \approx 0.4\%$. The calorimeter covers 98% of the solid angle and is composed by a barrel and two endcaps, for a total of 88 modules. Each module is read out at both ends by photomultipliers for a total of 2440 cells arranged in five layers. The energy deposits are obtained from the signal amplitude, while the arrival times and particles impact points are obtained from the spatial coordinates of the fired cell and the time differences. Cells close in time and space are grouped into energy clusters. The cluster energy E is calculated as the sum of the cell energies, while the cluster time T and position $\vec{R}$ are energy weighted averages. Energy and time resolutions are parametrized as $\sigma_E/E = 5.7\%/\sqrt{E\ (\mathrm{GeV})}$ and $\sigma_t = 57\ \mathrm{ps}/\sqrt{E\ (\mathrm{GeV})} \oplus 100$ ps, respectively. The trigger [8] uses both calorimeter and chamber information. In this analysis events are selected with the calorimeter trigger, requiring two energy deposits with $E > 50$ MeV for the barrel and $E > 150$ MeV for the endcaps. Data are then analyzed by an event classification filter [9], which selects and streams various categories of events in different output files.

In this Letter, we refer only to data collected during 2004–2005 for an integrated luminosity $\mathcal{L} = 1.7\ \mathrm{fb}^{-1}$ with the most stable running conditions and the best peak luminosity. A total of 5.1 billion ϕ mesons were produced, yielding 1.7×10^9 $K_S K_L$ pairs. Assuming $\mathrm{BR}(K_S \to 3\pi^0) \sim 1.9 \times 10^{-9}$ about 3 signal events are expected to have been produced.

3. Event selection

At DAΦNE the mean decay length of K_L, λ_L, is equal to ~ 340 cm and about 50% of K_L's reach the calorimeter before decaying. A very clean K_S tag is provided by the K_L interaction in the calorimeter (K_L-crash), which is identified by a cluster with polar angle $40^\circ < \theta_{cr} < 140^\circ$, not associated to any track, with energy $E_{cr} > 100$ MeV and with a time corresponding to a K_L velocity in the ϕ rest frame β^* in the range $[0.17, 0.28]$. The average value of the e^+e^- center of mass energy W is obtained with a precision of 20 keV for each 200 nb^{-1} running period using large angle Bhabha scattering events [3]. The value of W and the K_L-crash cluster position allows us to obtain, for each event, the direction of the K_S with an angular resolution of 1° and a momentum resolution of about 2 MeV.

Because of its short decay length, $\lambda_S \sim 0.6$ cm, the displacement of the K_S from the ϕ decay position is negligible. We therefore identify as photons from K_S decay, neutral particles that travel with $\beta = 1$ from the interaction point to the EMC ("prompt photons"). In order to retain a large control sample for the background while preserving high efficiency for the signal, we keep all photons satisfying $E_\gamma > 7$ MeV and $|\cos\theta| < 0.915$. Each cluster is required to satisfy the condition $|t_\gamma - R_\gamma/c| < \min(3.5\sigma_t, 2\ \mathrm{ns})$, where t_γ is the photon flight time and R the path length; σ_t also includes a contribution from the finite bunch length (2–3 cm), which introduces a dispersion in the collision time. The photon detection efficiency of the calorimeter amounts to about 90% for $E_\gamma = 20$ MeV, and reaches 100% above 70 MeV. After tagging the signal sample is selected requiring 6 prompt photons. For normalization we use the $K_S \to 2\pi^0$ decay which is selected requiring 4 prompt photons.

For both channels the expected background as well as the detector acceptance and the analysis efficiency are estimated using the Monte Carlo simulation of the experiment [9]. The simulation incorporates a detailed geometry and material composition of the KLOE apparatus and most of the data taking conditions of the experiment e.g. DAΦNE background rates, position of the interaction point and beam parameters. All the processes contributing to the background were simulated with statistics twice larger than the data sample. Moreover, for the acceptance and the analysis efficiency evaluation a dedicated $K_S \to 3\pi^0$ signal simulation was

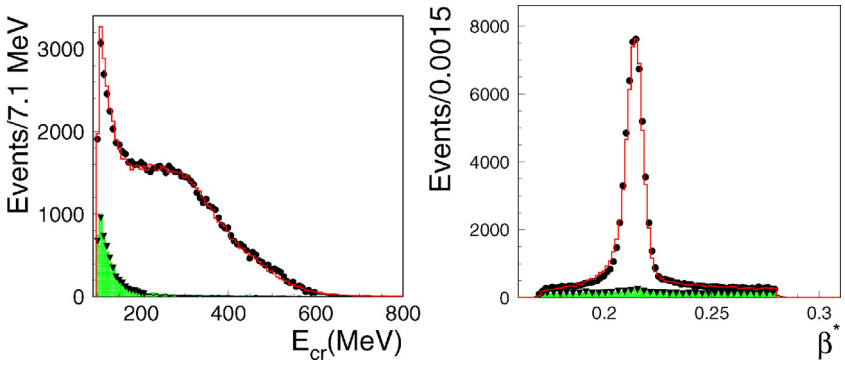

Fig. 1. Distributions of the K_L energy deposit in the EMC (E_{cr}) and velocity in the ϕ center of mass frame (β^*) for all events in the six-photon sample. Black points represent data, while the MC background simulation is shown as red histogram. The same distributions for events rejected by the track veto are shown by the black triangles (data) and green filled histograms (MC simulation). (For interpretation of the references to color in this figure legend, the reader is referred to the web version of this Letter.)

performed, based on a branching ratio equal to the best known upper limit [4] increased by a factor of 30 (about 5000 events).

3.1. The six-photon sample

The selection of the $K_S \to 3\pi^0$ decay is performed by asking for a K_L-crash and by searching six prompt photons from the decay of pions. After these requirements we count 76 689 events. For these events we perform further discriminant analysis to increase the signal to background ratio.

The first analysis step aims to reject fake K_S tags (about 2.5% of the total background). The distributions of E_{cr} and β^* for the selected data sample and background simulations are shown in Fig. 1. In the β^* distribution, the peak around 0.215 corresponds to genuine K_L interaction in the calorimeter, while the flat distribution mainly originates from $\phi \to K_S K_L \to (K_S \to \pi^+\pi^-, K_L \to 3\pi^0)$ background events. In this case one of the low momentum charged pions spirals in the forward direction and interacts in the low-β quadrupoles. This interaction produces neutral particles which simulate the signal of K_L interaction in the calorimeter (fake K_L-crash), while the K_L meson decays close enough to the interaction point to produce six prompt photons. To suppress fake K_L-crash we first reject events having charged particles produced close to the interaction region (track veto). The distributions of the kinematical variables for the vetoed background events are shown in Fig. 1. Taking advantage of the differences in the β^* and E_{cr} distributions between the tagged K_S events and the fake K_L-crash, we have tightened the cuts on these variables: $E_{cr} > 150$ MeV and $0.20 < \beta^* < 0.225$ (K_L-crash hard). This improves by a factor 12 the rejection of this background with respect to the previous analysis [4].

The second source of background originates from wrongly reconstructed $K_S \to 2\pi^0$ decays. The four photons from this decay can be reconstructed as six due to fragmentation of the electromagnetic showers (splitting). These events are characterized by one or two low-energy clusters reconstructed very close to the position of the genuine photon interaction in the calorimeter and constitute about 67.5% of the background. Additional clusters come from accidental time coincidence between ϕ decay and machine background photons from DAΦNE ($\sim 30\%$ of the background). After tagging with the K_L-crash hard algorithm and applying the track veto we remain with a sample of about 50 000 six-photon events. A kinematic fit with 11 constraints has been performed imposing energy and momentum conservation, the kaon mass and the velocity of the six photons in the final state. The χ^2 distribution of the fit for data and background simulation, χ^2_{fit}, is shown in Fig. 2 together with the expected distribution for signal events. Cutting on

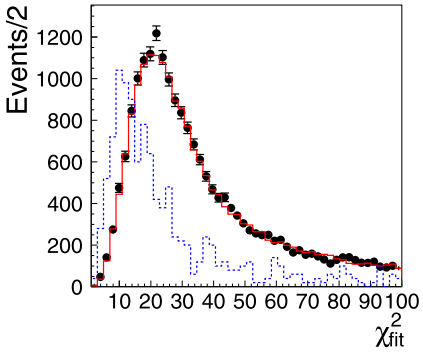

Fig. 2. Distribution of χ^2_{fit} for the tagged six-photon sample for data (black points), background simulation (solid histogram), and simulated $K_S \to 3\pi^0$ signal (dashed histogram).

χ^2_{fit} reduces by about 30% the remaining background while keeping the signal efficiency at 70% level.

In order to improve rejection of events with split and accidental clusters, we have exploited the correlation between two χ^2-like variables named $\zeta_{2\pi}$ and $\zeta_{3\pi}$. $\zeta_{2\pi}$ is calculated by an algorithm selecting the best four out of six clusters satisfying the kinematic constraints of the two-body decay in the $K_S \to 2\pi^0 \to 4\gamma$ hypothesis:

$$\zeta_{2\pi} = \frac{(m_{1\gamma\gamma} - m_{\pi^0})^2}{\sigma^2_{2\pi}} + \frac{(m_{2\gamma\gamma} - m_{\pi^0})^2}{\sigma^2_{2\pi}} + \frac{(\theta_{\pi\pi} - \pi)^2}{\sigma^2_{\theta_{\pi\pi}}} + \frac{(E_{K_S} - \sum_{i=1}^4 E_{\gamma_i})^2}{\sigma^2_{E_{K_S}}} + \frac{(p^x_{K_S} - \sum_{i=1}^4 p^x_{\gamma_i})^2}{\sigma^2_{p_x}} + \frac{(p^y_{K_S} - \sum_{i=1}^4 p^y_{\gamma_i})^2}{\sigma^2_{p_y}} + \frac{(p^z_{K_S} - \sum_{i=1}^4 p^z_{\gamma_i})^2}{\sigma^2_{p_z}}, \quad (1)$$

where $m_{1\gamma\gamma}$ and $m_{2\gamma\gamma}$ are the reconstructed $\gamma\gamma$ masses for a given cluster pairing, and $\theta_{\pi\pi}$ denotes the opening angle of the reconstructed pion directions in the K_S center of mass frame. E_{K_S} and p_{K_S} stand for the K_S energy and momentum vector determined from the reconstructed four-momentum of K_L, while E_{γ_i} and p_{γ_i} are energies and momenta of four out of six reconstructed photons. The minimization of $\zeta_{2\pi}$ gives the best two photon pairs fulfilling the $K_S \to 2\pi^0 \to 4\gamma$ hypothesis. The resolutions used in Eq. (1) were estimated independently on data and MC simulation using a $K_S \to 2\pi^0 \to 4\gamma$ control sample.

The second χ^2-like variable, $\zeta_{3\pi}$, instead verifies the signal hypothesis $K_S \to 3\pi^0$ by looking at the reconstructed masses of the three pions. For each pair of clusters we evaluate $\zeta_{3\pi}$ as:

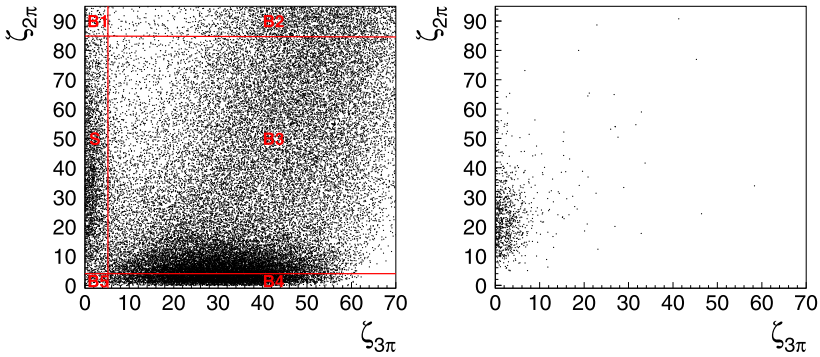

Fig. 3. Distributions of events in the $\zeta_{3\pi}$–$\zeta_{2\pi}$ plane, for six-photon sample tagged by K_L-crash for data (left), and for the simulated $K_S \to 3\pi^0$ decays (right). The boundaries of the background control regions B1, B2, B3, B4, B5 and the signal region S are as specified in the text.

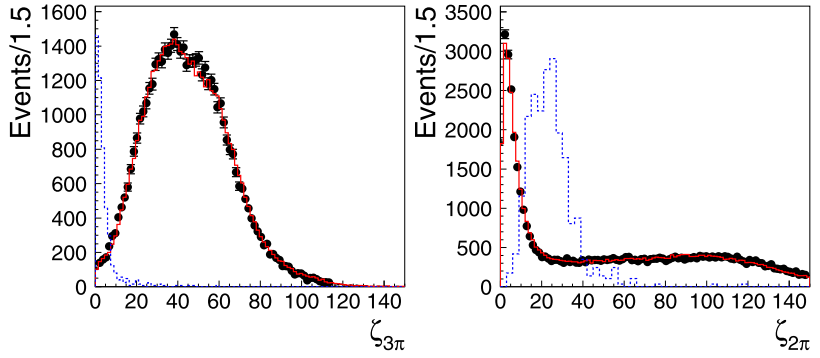

Fig. 4. Inclusive distributions of the $\zeta_{3\pi}$ and $\zeta_{2\pi}$ discriminating variables for six-photon events: data (black points), background simulations (red curves). The dashed histograms represents simulated $K_S \to 3\pi^0$ events. (For interpretation of the references to color in this figure legend, the reader is referred to the web version of this Letter.)

Table 1
Number of events populating control regions in the $\zeta_{3\pi}$–$\zeta_{2\pi}$ plane defined in Fig. 3 after tight requirements on K_L-crash and track veto.

	SBOX	B1	B2	B3	B4	B5
DATA	220 ± 15	5 ± 3	$15\,179 \pm 123$	$26\,491 \pm 163$	6931 ± 83	137 ± 12
MC	239 ± 11	4 ± 3	$14\,905 \pm 116$	$26\,964 \pm 169$	6797 ± 76	100 ± 7

$$\zeta_{3\pi} = \frac{(m_{1\gamma\gamma} - m_{\pi^0})^2}{\sigma_{3\pi}^2} + \frac{(m_{2\gamma\gamma} - m_{\pi^0})^2}{\sigma_{3\pi}^2} + \frac{(m_{3\gamma\gamma} - m_{\pi^0})^2}{\sigma_{3\pi}^2}. \quad (2)$$

As the best combination of cluster pairs, we take the configuration minimizing $\zeta_{3\pi}$. The resolution on the $\gamma\gamma$ invariant mass in the $3\pi^0$ hypothesis, $\sigma_{3\pi}$, was estimated applying the algorithm to the simulated $K_S \to 3\pi^0$ events.

The distributions in the $\zeta_{3\pi}$–$\zeta_{2\pi}$ plane for the data and $K_S \to 3\pi^0$ simulated signal are shown in Fig. 3. Signal events are characterized by small values of $\zeta_{3\pi}$ and relatively high $\zeta_{2\pi}$. To compare data and Monte Carlo simulations we have subdivided the $\zeta_{3\pi}$–$\zeta_{2\pi}$ plane into six regions B1, B2, B3, B4, B5, and S as indicated in the left panel of Fig. 3. Region S, with the largest signal-to-background ratio, is the signal box, while B1–B5 are control regions used to check the reliability of the simulation and optimize our description of the experimental data.

Simulation does not reproduce accurately the absolute number of events belonging to different background categories. However, their kinematical properties are reproduced quite well. To determine the background composition, and improve the description of experimental data, we have performed a binned likelihood fit of a linear combination of simulated $\zeta_{3\pi}$–$\zeta_{2\pi}$ distributions to the same data distribution for all background categories. The quality of the fit was controlled by comparing inclusive distributions of discriminating variables between data and simulation. Examples are presented in Fig. 4.

Table 1 shows the comparison of observed number of events with the expectations in each control region of the $\zeta_{3\pi}$–$\zeta_{2\pi}$ plane. The agreement is better than 1.5σ in all regions except region B5 (2.8σ).

To further improve the $K_S \to 2\pi^0$ background rejection we cut on the Δ variable defined as:

$$\Delta = \left(m_\phi/2 - \sum E_{\gamma_i}\right)/\sigma_E, \quad (3)$$

where $\sum E_{\gamma_i}$ is the sum of energies of the four prompt photons selected by the $\zeta_{2\pi}$ algorithm and σ_E stands for the 4γ energy resolution estimated using the $K_S \to 2\pi^0 \to 4\gamma$ control sample. For $K_S \to 2\pi^0$ decays with two additional background clusters, we expect $\Delta \sim 0$, while for $K_S \to 3\pi^0$ events $\Delta \sim m_{\pi^0}/\sigma_E$. To further reject surviving $K_S \to 2\pi^0$ events with split clusters, we cut on the minimal distance between centroids of reconstructed clusters, R_{min}, considering that the distance between split clusters is on average smaller than the distance between clusters originating from γ's of $K_S \to 3\pi^0$ decay. Distributions of these two discriminant variables are presented in Fig. 5.

Before opening the signal box, the cuts on the discriminant variables have been refined minimizing $f_{cut}(\chi^2_{fit}, \zeta_{2\pi}, \zeta_{3\pi}, \Delta, R_{min}) = N_{up}/\epsilon_{3\pi}$, where $\epsilon_{3\pi}$ stands for the signal efficiency

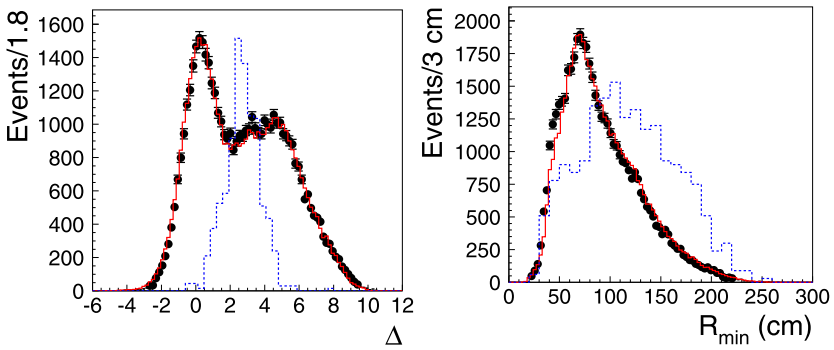

Fig. 5. Distributions of Δ and R_{min} discriminating variables for six-photon events: data (black points), background simulations (red curves). The dashed histograms represents simulated $K_S \to 3\pi^0$ events. (For interpretation of the references to color in this figure legend, the reader is referred to the web version of this Letter.)

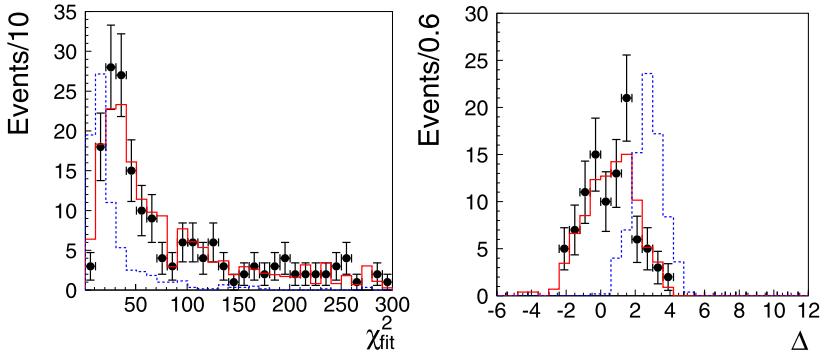

Fig. 6. Distributions of χ^2_{fit} for six-photon events in the signal box (left) and Δ for six-photon events in the signal box applying the $\chi^2_{fit} < 57.2$ cut (right). Black points are data, background simulation is the red histogram. The dashed histogram represents simulated $K_S \to 3\pi^0$ events. (For interpretation of the references to color in this figure legend, the reader is referred to the web version of this Letter.)

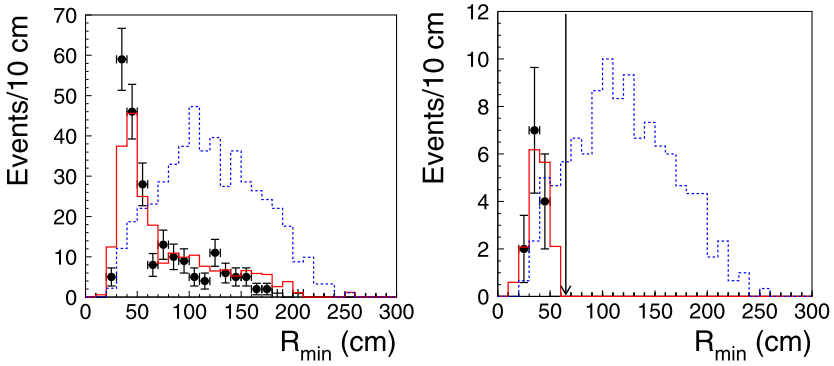

Fig. 7. Distributions of R_{min} for six-photon events in the signal box applying the $\chi^2_{fit} < 57.2$ cut (left), and applying $\chi^2_{fit} < 57.2$ and $\Delta > 1.88$ cuts (right). Black points are data, background simulation is the red histogram. The dashed histogram represents simulated $K_S \to 3\pi^0$ events. (For interpretation of the references to color in this figure legend, the reader is referred to the web version of this Letter.)

and N_{up} is the mean upper limit (at 90% C.L.) on the expected number of signal events calculated on the basis of the expected number of background events $B_{exp} = B_{exp}(\chi^2_{fit}, \zeta_{2\pi}, \zeta_{3\pi}, \Delta, R_{min})$ from simulation [11]. The outcome of the optimizing procedure is $\chi^2_{fit} < 57.2$, $\Delta > 1.88$ and $R_{min} > 65$ cm. The signal box is defined as: $4 < \zeta_{2\pi} < 84.9$ and $\zeta_{3\pi} < 5.2$. At each stage of the analysis we checked that the simulation describes the data within statistical uncertainty. Distributions of χ^2_{fit}, Δ and R_{min} variables are presented in Figs. 6 and 7 for events in the signal box. In the right panel of Fig. 7 we present also the R_{min} distribution just before the last cut $R_{min} > 65$ cm. According to the Monte Carlo simulation, these survived events are all $K_S \to 2\pi^0$ decays with two split clusters (95%), or one split and one accidental cluster (5%). A total efficiency of $\epsilon_{3\pi} = 0.233 \pm 0.012_{\rm stat}$ has been estimated. At the end of the analysis we find zero candidates in data and in the simulated background sample. To assign an error to the Monte Carlo estimate of the background, N_b, we have fit the simulated R_{min} distribution of Fig. 7 (right) with a gaussian and a log-gaussian. Integrating the events above the cut we estimated $N_b = 0.04^{+0.15}_{-0.03}$.

3.2. The normalization sample

The $K_S \to 2\pi^0$ normalization sample is selected requiring four prompt photons. The Monte Carlo simulation shows an amount of background of about 0.1% of the total. These events are essentially $\phi \to K^+K^-$ decays. After the K_L-crash hard tagging we find

Table 2
The probabilities to find one (P_{A1}) or two (P_{A2}) accidental clusters and to reconstruct one (P_{S1}) or more (P_{S2}) split clusters estimated using out of time clusters and fit to the photon multiplicities, as described in the text.

	P_{A1} [%]	P_{A2} [%]	P_{S1} [%]	P_{S2} [%]
DATA	0.378 ± 0.004	0.025 ± 0.001	0.30 ± 0.01	0.0103 ± 0.0001
MC	0.492 ± 0.004	0.027 ± 0.001	0.31 ± 0.01	0.0156 ± 0.0002

$N_{2\pi} = (7.533 \pm 0.018) \times 10^7$ events. With the Monte Carlo simulations we have also determined the $K_S \to 2\pi^0 \to 4\gamma$ efficiency: $\epsilon_{2\pi} = 0.660 \pm 0.002_{\text{stat}}$. The final number of produced $K_S \to 2\pi^0$ events is: $N_{\text{norm}} = N_{2\pi}/\epsilon_{2\pi} = (1.142 \pm 0.005) \times 10^8$.

3.3. Evaluation of systematic uncertainties

The systematic uncertainties are related to the number of background events and to the determination of the acceptance and total efficiencies for the signal, $\epsilon_{3\pi}$, and normalization, $\epsilon_{2\pi}$, samples.

For the tagged six-photon sample, we have investigated the uncertainties related to the observed background at the end of the analysis. A difference of $\sim 2.4\%$ in the EMC energy scale and resolution has been observed between data and MC simulation and has been studied using a control sample of $K_S \to 2\pi^0$ events. To evaluate the related systematic uncertainty on the background, we have repeated the upper limit evaluation with several values of the energy scale correction in the range of 2.2%–2.6%. Similarly, the analysis has been repeated modifying the resolution used in the definition of $\zeta_{2\pi}$ and $\zeta_{3\pi}$. Moreover, we have varied of 1σ the resolution used in the Δ variable calculation and removed a data–MC shift correction on R_{min}. These variations correspond to a cut change of 5% and 6%, respectively. Similarly, we have removed the data–MC scale correction for E_{cr} and the additional gaussian smearing in the MC β^* distribution, both corresponding to a 5% variation of the cuts. The full analysis was repeated in total twenty times applying each time one of the changes mentioned above. For all of these checks, we have observed no variation in the number of simulated background.

For the acceptance of both the signal and normalization samples, we have evaluated the systematic uncertainty on the photon counting by comparing data and simulation splitting, accidental probabilities and cluster reconstruction efficiency. To determine the probabilities of one, P_{A1}, or two, P_{A2}, accidental clusters in the event we have used out of time clusters originated from earlier bunch crossing. To estimate the probability of generating one, P_{S1}, or more fragments, P_{S2}, per cluster, we have fit the photon multiplicities observed in data using the experimental values of P_{A1} and P_{A2}, and the photon multiplicities obtained by the simulation [12,13]. Results of these fits are reported in Table 2. The photon reconstruction efficiency, for both data and MC, was evaluated using a control sample of $\phi \to \pi^+\pi^-\pi^0$ events. The momentum of one of the photons is estimated from tracking information and position of the other cluster. The candidate photon is then searched for within a search cone. The systematic error related to the cluster efficiency has been estimated by removing the data/MC efficiency correction. The total systematic uncertainty on the acceptance for both measured samples is listed in Table 3. Another source of systematic uncertainties originates from the offline filter FILFO [14] used, during data reconstruction, to reject cosmic rays and machine background events before starting the track reconstruction. The FILFO efficiency, for both normalization and signal samples, has been estimated using the simulation and is very close to 100% [12]. We have conservatively assigned as systematic uncertainty in data half of the difference between the MC evaluated efficiency and 100%. We consider completely negligible the influence of trigger efficiency for both samples, since in [4] it was about 99.5% and the K_L-crash hard tagging requires a larger energy release in the calorimeter, which translates in a larger trigger efficiency.

Table 3
Summary table of the systematic uncertainties on the total efficiencies for the signal, $\epsilon_{3\pi}$, and normalization samples, $\epsilon_{2\pi}$.

Source	$\Delta\epsilon_{2\pi}/\epsilon_{2\pi}$ [%]	$\Delta\epsilon_{3\pi}/\epsilon_{3\pi}$ [%]
Acceptance	1.60	0.21
Offline filter	0.46	0.30
Calorimeter energy scale	–	1.00
Calorimeter energy resolution	–	1.10
χ^2_{fit} cut	–	1.46
R_{min} cut	–	0.90
TOTAL	1.65	2.30

The observed difference in the EMC energy scale and resolution between data and simulation enters also in the $\epsilon_{3\pi}$ evaluation. The effects have been estimated as $\Delta\epsilon_{3\pi}/\epsilon_{3\pi} = 1.0\%$ from the energy scale, and $\Delta\epsilon_{3\pi}/\epsilon_{3\pi} = 1.1\%$ from the resolution. The effect of the cut on χ^2_{fit} has been tested constructing the ratio between the cumulative distributions for experimental data and simulation which leads to a systematics of $\Delta\epsilon_{3\pi}/\epsilon_{3\pi} = 1.46\%$. Finally, we have investigated the systematic effect related to the R_{min} cut by varying its value by 6%, and estimated its contribution to be $\Delta\epsilon_{3\pi}/\epsilon_{3\pi} = 0.9\%$.

All the contributions to the systematic uncertainty are summarized in Table 3, with the total systematic uncertainty evaluated adding all effects in quadrature.

4. Results

No events were observed on data in the signal region. Equally, no background events are found in the MC simulation based on twice the data statistics. In the conservative assumption of no background, we estimate an upper limit on the expected number of signal events $\text{UL}(\text{Nev}(K_S \to 3\pi^0)) = 2.3$ at 90% C.L., with a signal efficiency of $\epsilon_{3\pi} = 0.233 \pm 0.012_{\text{stat}} \pm 0.006_{\text{sys}}$. In the same tagged sample we count $N_{\text{norm}} = (1.142 \pm 0.005) \times 10^8$ $K_S \to 2\pi^0$ events.

Systematic uncertainties on background determination, as well as on the efficiency evaluation for the signal and normalization samples, are negligible in the calculation of the limit.

Using the value $\text{BR}(K_S \to 2\pi^0) = 0.3069 \pm 0.0005$ [10] we obtain:

$$\text{BR}\left(K_S \to 3\pi^0\right) \leqslant 2.6 \times 10^{-8} \quad \text{at 90\% C.L.} \tag{4}$$

which represents the best limit on this decay, improving by a factor of ~ 5 previous result [4].

This result can be translated into a limit on $|\eta_{000}|$:

$$\begin{aligned} |\eta_{000}| &= \left| \frac{A(K_S \to 3\pi^0)}{A(K_L \to 3\pi^0)} \right| \\ &= \sqrt{\frac{\tau_L}{\tau_S} \frac{\text{BR}(K_S \to 3\pi^0)}{\text{BR}(K_L \to 3\pi^0)}} \\ &\leqslant 0.0088 \quad \text{at 90\% C.L.} \end{aligned} \tag{5}$$

This describes a circle of radius 0.0088 centered at zero in the $\Re(\eta_{000})$, $\Im(\eta_{000})$ plane and represents a limit two times smaller than previous result [4].

Acknowledgements

We warmly thank our former KLOE colleagues for the access to the data collected during the KLOE data taking campaign. We thank the DAΦNE team for their efforts in maintaining low background running conditions and their collaboration during all data taking. We want to thank our technical staff: G.F. Fortugno and F. Sborzacchi for their dedication in ensuring efficient operation of the KLOE computing facilities; M. Anelli for his continuous attention to the gas system and detector safety; A. Balla, M. Gatta, G. Corradi and G. Papalino for electronics maintenance; M. Santoni, G. Paoluzzi and R. Rosellini for general detector support; C. Piscitelli for his help during major maintenance periods.

We acknowledge the support of the European Community – Research Infrastructure Integrating Activity 'Study of Strongly Interacting Matter' (acronym HadronPhysics2, Grant Agreement No. 227431) under the Seventh Framework Programme of EU. This work was supported also in part by the EU Integrated Infrastructure Initiative Hadron Physics Project under contract number RII3-CT-2004-506078; by the European Commission under the 7th Framework Programme through the 'Research Infrastructures' action of the 'Capacities' Programme, Call: FP7-INFRASTRUCTURES-2008-1, Grant Agreement No. 283286; by the Polish National Science Centre through the Grants Nos. 0469/B/H03/2009/37, 0309/B/H03/2011/40, DEC-2011/03/N/ST2/02641, 2011/01/D/ST2/00748, 2011/03/N/ST2/02652, 2011/03/N/ST2/02641 and by the Foundation for Polish Science through the MPD programme and the project HOMING PLUS BIS/2011-4/3.

References

[1] G. D'Ambrosio, et al., in: L. Maiani, et al. (Eds.), The Second DAΦNE Handbook, Frascati, 1995, p. 63.
[2] A. Lai, et al., Phys. Lett. B 610 (2005) 165.
[3] F. Bossi, E. De Lucia, J. Lee-Franzini, S. Miscetti, M. Palutan, Riv. Nuovo Cim. 31 (2008) 531.
[4] F. Ambrosino, et al., Phys. Lett. B 619 (2005) 61.
[5] G.V. Vignola, S. Bartalucci, M. Bassetti, M.E. Biagini, C. Biscari, R. Boni, A. Cattoni, V. Chimenti, et al., Conf. Proc. C 930517 (1993) 1993.
[6] M. Adinolfi, et al., Nucl. Inst. and Meth. A 488 (2002) 51.
[7] M. Adinolfi, et al., Nucl. Inst. and Meth. A 482 (2002) 364.
[8] M. Adinolfi, et al., Nucl. Inst. and Meth. A 492 (2002) 134.
[9] F. Ambrosino, et al., Nucl. Inst. and Meth. A 534 (2004) 403.
[10] J. Beringer, et al., Particle Data Group Collaboration, Phys. Rev. D 86 (2012) 010001.
[11] J.F. Grivaz, F. Le Diberder, LAL-92-37, 1992.
[12] M. Silarski, arXiv:1302.4427 [hep-ex].
[13] M. Martini, S. Miscetti, Determination of the probability of accidental coincidence between machine background and collision events and fragmentation of electromagnetic showers, KLOE note 201, http://www.lnf.infn.it/kloe, 2005.
[14] M. Moulson, S.E. Müller, FILFO revisited: A new look at the offline reconstruction filter and event classification, KLOE Memo 288, http://www.lnf.infn.it/kloe, 2004.